Uptake of Fluorine-18-Fluorodeoxyglucose in Sarcoidosis

Petra J. Lewis and Alan Salama

The Clinical PET Centre, Guy's & St. Thomas' Hospital and Department of Thoracic Medicine, Guy's Hospital, London

Whole-body PET scanning was performed using ^{18}F-fluorodeoxyglucose (FDG) in two patients with hilar lymphadenopathy in whom the clinical differential diagnosis was between sarcoidosis and lymphoma. Both patients were later proven to have sarcoidosis. Uptake of ^{18}FDG was seen in both intra- and extrathoracic lesions as well as in associated erythema nodosum. One patient underwent a repeat scan after steroid therapy where a marked decrease in hilar uptake was seen. Fluorine-18-fluorodeoxyglucose uptake is observed in lymph nodes with sarcoid involvement. Further investigation is necessary to assess if quantitative differences exist between sarcoid and malignant lymphadenopathy.

Key Words: sarcoidosis; fluorine-18-fluorodeoxyglucose; lymphadenopathy

J Nucl Med 1994; 35:1647–1649

A common clinical and radiographic diagnostic problem is the differentiation between sarcoidosis and lymphoma in patients presenting with hilar lymphadenopathy. Differentiation between the two diseases can be difficult in some patients, often requiring mediastinoscopy and biopsy. As ^{18}FDG has been used in clinical PET to differentiate benign and malignant lesions (*1–4*) and several studies have shown avid ^{18}FDG uptake in both Hodgkins and non-Hodgkin's lymphoma (*1,5–8*) this might potentially be an area where whole-body ^{18}FDG PET scanning may provide useful information. We report on two patients with active sarcoidosis where significant ^{18}FDG accumulation was seen on whole-body ^{18}FDG PET scanning.

CASE REPORTS

All studies were acquired on an ECAT 951 whole-body PET system (Siemens/CTI Knoxville TN) which produces 31 slices over a 10.6 cm axial field of view. The intrinsic resolution before reconstruction is 6 mm transaxially and 4.5 mm axially centrally. Patients were scanned 40 min following intervenous injection of 250 MBq ^{18}FDG. Whole-body images were obtained by acquiring 10 consecutive 5 min images from the patient's head to below the pelvis. In patient 2, a further 5 sets of images were acquired to include the remainder of the lower limbs. The complete sets of 310 (450) image planes were reconstructed and smoothed in the axial direction to obtain a single 3D dataset with the same spatial resolution of 12 mm in x, y and z, directions.

Patient 1

A 46-yr-old nonsmoking obese Asian female presented with a 2 mo history of shortness of breath, nocturnal sweats, rigors, left-sided chest pains and dysphonia. She had bilateral scattered inspiratory and expiratory wheezes and a small palpable left cervical lymph node. Chest radiography showed prominent paratracheal and hilar shadows with normal lung parenchyma. Sputum was negative for acid fast bacilli (AFBs) and a bronchoscopy revealed a bulging carina with externally compressed bronchi. Bronchoalveolar lavage revealed a lymphocytosis (18%, N < 15), with no evidence of malignancy or tuberculosis. Respiratory function tests (RFTs) revealed a restrictive lung defect. CT showed extensive superior mediastinal, paratracheal and carinal adeno-pathy with hepatosplenomegaly which was felt to be highly suggestive of lymphoma and she was referred for a whole-body ^{18}FDG PET scan.

The PET study (Fig. 1) shows multiple areas of intense ^{18}FDG uptake including the hilar and paratracheal regions bilaterally, paraaortic region, cervical region bilaterally, inguinal regions bilaterally, left axilla and the right lobe of the liver. The spleen was also enlarged with increased ^{18}FDG uptake. Inguinal nodes could not be palpated due to the patient's marked obesity.

Mediastinoscopy and lymph node biopsy was performed, histology showed granulomas with no evidence of malignant cells, caeseation or acid fast bacilli. A diagnosis of sarcoidosis was made and she was treated with oral steroids making a good recovery.

Patient 2

A 30-yr-old caucasian nonsmoking male presented with a three wk history of large joint arthralgia, malaise, night sweats and cough. He had multiple raised indurated lesions on his lower limbs consistent with erythema nodosum. Blood tests showed a raised erythrocyte sedimentation rate (ESR) at 115 mm/hr, C-reactive protein 18.2 (normal <1.0) and alanine amino transferase 139 (normal <55). Viral titers, hepatitis screen, electrolytes and Mantoux test were normal. Chest radiography showed bilateral hilar lymphadenopathy. A skin biopsy was in keeping with erythema nodosum. RFTs showed a restrictive defect. Bronchoscopy was normal and bronchioalveolar lavage showed 42% lymphocytes, 55% macrophages.

Received Jul. 26, 1993; revision accepted Jan. 26, 1994.

For correspondence or reprints contact: Dr. Petra Lewis, The Clinical PET Centre, Lower Ground Floor, Lambeth Wing, St. Thomas' Hospital, Lambeth Palace Rd., London SE1 7EH, England.

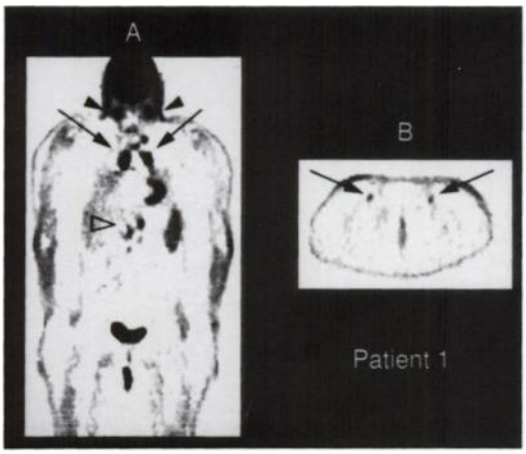

FIGURE 1. Whole-body ^{18}FDG scan of Patient One: (A) Coronal slice through the lung hilum showing intense ^{18}FDG uptake by hilar lymphnodes (arrow), cervical lymphnodes (arrow head) and paraaortic nodes (open arrowhead). Increased splenic uptake is also seen. (B) Transaxial slice through the groin shows uptake in inguinal lymphnodes.

A whole-body ^{18}FDG PET scan on the patient (Fig. 2) showed massively increased ^{18}FDG uptake in the hilar and paratracheal regions with patchy superficial uptake over both lower limbs. The patient was treated with oral steroids with the presumptive diagnosis of sarcoidosis based on clinical grounds and markedly improved after 3 mo. He underwent a second ^{18}FDG PET scan at this point, when his only complaint was of lower limb muscle pain. This scan (Fig. 3) showed complete resolution of the hilar and cutaneous uptake, but intense FDG uptake throughout the muscles of the lower limbs, maximal in the calf muscles. At this time, ESR = 4 mm/hr, and creatinine phosphokinase was normal.

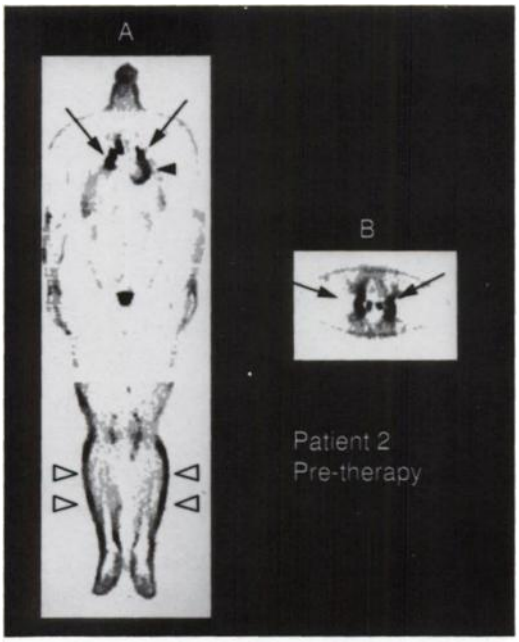

FIGURE 2. Whole-body ^{18}FDG scan of Patient Two: (A) Coronal and (B) transaxial slice through the lung hilum showing intense ^{18}FDG uptake by hilar lymphnodes (arrow) as well as uptake into erythema nodosum on the lower limbs (open arrowhead). The heart is indicated by the closed arrowhead.

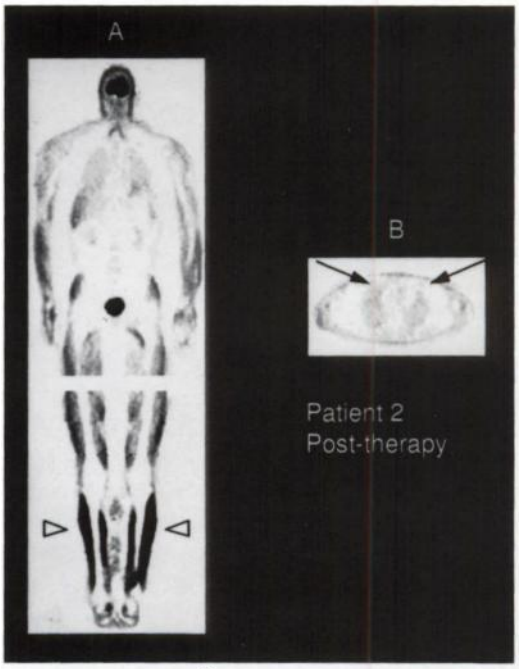

FIGURE 3. Whole-body ^{18}FDG scan of Patient Three after steroid therapy: (A) Coronal and (B) transaxial slice through the lung hilum showing resolution of hilar uptake (arrow), but intense muscle uptake seen in the lower limbs (open arrowhead). The heart is indicated by the closed arrowhead.

DISCUSSION

The PET ^{18}FDG literature has previously suggested that significant uptake of ^{18}FDG in lymph nodes is indicative of malignant neoplastic tissue including lymphoma (*1,5,7,8*). ^{18}FDG PET scanning is therefore increasingly being proposed as a method to differentiate benign and malignant lesions in the thorax (*3,9,10*). No report to date has been published on patients with sarcoidosis using the whole-body PET scanning technique (*11*). Valind et al. reported finding increased ^{18}FDG uptake in the lung parenchyma of three patients with pulmonary sarcoidosis (*12*) and Kubota et al. reported ^{18}FDG uptake in a pulmonary granuloma (*3*).

Gallium-67-citrate has been widely used and studied in single photon scanning in both sarcoidosis (*13–16*) and lymphoma (*17–20*). These studies have described typical patterns of ^{67}Ga uptake in sarcoidosis, perhaps the best described being the 'lambda' pattern of mediastinal lymphadenopathy, which some authors have found to be highly sensitive for sarcoidosis (*15*), although others disagree (*16*). Both of our patients had hilar and right paratracheal lymph node ^{18}FDG uptake which conformed to the lambda pattern. The 'panda' pattern of lacrimal, parotid and nasal uptake, also described in a significant proportion of patients with sarcoidosis (*15*), may be seen in other conditions including Sjögrens, rheumatoid arthritis and CMV infection (*21*). Neither of our subjects demonstrated abnormal uptake of ^{18}FDG in lacrimal or parotid glands or in the nasal mucosa.

Both of our patients had hilar lymphadenopathy, one also had extrapulmonary lymph node involvement and one erythema nodosum. All lesions were found to markedly accumulate ^{18}FDG, including the erythema nodosum. The pattern of extrathoracic lymph node involvement seen in patient one is rarely seen in gallium scans of patients with sarcoidosis, and would be more typical of lymphoma (*15,16*). We suggest that the cellular uptake of ^{18}FDG in these patients is related to inflammatory cell infiltrate; ^{18}FDG has been seen in vitro to be accumulated by leukocytes (*22*), lymphocytes and macrophages (*23,24*) and ^{18}FDG uptake may be seen in vivo at sites of infection (*25*). In sarcoidosis the cellular infiltrate is composed of lymphocytes, macrophages and epithelioid cells (from monocytes) (*26*), inflammatory cells are also present in erythema nodosum. This is consistent with the absence of hilar ^{18}FDG uptake following successful steroid therapy in patient two and it is possible that ^{18}FDG PET may provide a means, albeit expensive, of assessing disease activity. The muscle uptake seen in this patient in connection with the lower limb pains may indicate that the patient was suffering from a sarcoid myopathy or myositis which is a reported, although uncommon site of sarcoid involvement (*27,28*). Uptake of ^{67}Ga by muscles involved in sarcoidosis has also been reported (*29,30*). Our patient had not undergone vigorous exercise prior to ^{18}FDG injection, which could be an alternative explanation for this appearance.

Our findings of ^{18}FDG uptake in sarcoidosis in conjunction with those of Valind and Kubota (*3,12*) suggest that the use of PET ^{18}FDG whole-body scanning to differentiate between sarcoidosis and lymphoma may be considerably limited. Physicians should be aware of this nonspecificity when using ^{18}FDG PET scanning to assess hilar lymphadenopathy. Further prospective studies are required to assess and compare the intensity and patterns of ^{18}FDG uptake in sarcoidosis and lymphoma, with comparison to ^{67}Ga scanning. Whole-body imaging with ^{18}FDG could potentially be used to assess the extent of sarcoidosis. This approach should be compared to the much less expensive and readily available option of ^{67}Ga.

ACKNOWLEDGMENTS

We thank Dr. J. Rees and Dr. G.M. Cochrane who referred the patients for this study, and Angela Dynes and John Lowe for technical support.

REFERENCES

1. Hoffman JM, Waskin HA, Schifter T, Hanson MW, Coleman RE. The use of FDG-PET in differentiating infectious from malignant central nervous system lesions in patients with AIDS. *J Nucl Med* 1992;33:838.
2. Griffeth LK, Dehdashti F, McGuire AH, et al. PET evaluation of soft-tissue masses with fluorine-18 fluoro-2-deoxy-D-glucose. *Radiology* 1992;182:185–194.
3. Kubota K, Matsuzawa T, Fujiwara T, et al. Differential diagnosis of lung tumour with positron emission tomography: a prospective study. *J Nucl Med* 1990;31:1927–1932.
4. Strauss LG, Clorius JH, Schlag P, et al. Recurrence of colorectal tumors: PET evaluation. *Radiology* 1989;170:329–332.
5. Okada J, Yoshikawa K, Itami M, et al. Positron emission tomography using fluorine-18-fluorodeoxyglucose in malignant lymphoma: a comparison with proliferative activity. *J Nucl Med* 1992;33:325–329.
6. Rosenfeld SS, Hoffman JM, Coleman RE, Glantz MJ, Hanson MW, Schold SC. Studies of primary central nervous system lymphoma with fluorine-18-fluorodeoxyglucose positron emission tomography. *J Nucl Med* 1992;33:532–536.
7. Leskinen Kallio S, Ruotsalainen U, Nagren K, Teras M, Joensuu H. Uptake of carbon-11-methionine and fluordeoxyglucose in non-Hodgkin's lymphoma: a PET study. *J Nucl Med* 1991;32:1211–1218.
8. Okada J, Yoshikawa K, Imazeki K, et al. The use of FDG-PET in the detection and management of malignant lymphoma: correlation of uptake with prognosis. *J Nucl Med* 1991;32:686–691.
9. Patz EF, Lowe VJ, Hoffman JM, et al. Focal pulmonary abnormalities: evaluation with ^{18}F-fluorodeoxyglucose PET scanning. *Radiology* 1993;188:487–490.
10. Knopp MV, Bischoff H, Ostertag H, et al. Clinical applications of FDG-PET for staging of bronchogenic carcinoma. *J Nucl Med* 1993;34:21P.
11. Dahlborn M, Hoffman EJ, Hoh CK, et al. Whole-body positron emission tomography: Part 1. Methods and performance characteristics. *J Nucl Med* 1991;33:1191–1199.
12. Valind SO, Rhodes CG, Paltin C, Suzuki T, Hughes JMB. Measurements of pulmonary glucose metabolism in patients with cryptogenic fibrosing alveolitis and pulmonary sarcoidosis. *Am Rev Respir Dis* 1984;129:A53.
13. Beckerman C, Hoffer PB, Bitran JD, Gupta RG. Gallium-67 citrate imaging studies of the lung. *Semin Nucl Med* 1980;10:286–301.
14. Alavi A, Palevsky HI. Gallium-67-citrate scanning in the assessment of disease activity in sarcoidosis. *J Nucl Med* 1992;33:751–755.
15. Sulavik SB, Spencer RP, Weed DA, Shapiro HR, Shiue S, Castriotta RJ. Recognition of distinctive patterns of gallium-67 distribution in sarcoidosis. *J Nucl Med* 1990;31:1909–1914.
16. Israel HI, Albertine KH, Park CH, Patrick H. Whole-body gallium 67 scans. *Am Rev Respir Dis* 1991;144:1182–1186.
17. Front S, Ben Haim S, Israel O, et al. Lymphoma: predictive value of Ga-67 scintigraphy after treatment. *Radiology* 1992;182:359–363.
18. King DJ, Dawson AA, McDonald AF. Gallium scanning in lymphoma. *Clin Radiol* 1980;31:729–732.
19. Turner DA, Fordham EW, Ali A, Slayton RE. Gallium-67 imaging in the management of Hodgkin's disease and other malignant lymphomas. *Semin Nucl Med* 1978;8:205–218.
20. Fox K, Silfen D, Alavi A. Applications of gallium-67 scintigraphy in the management of patients with malignant lymphoma. *J Nucl Med* 1991;32:2299–2305.
21. Brown ML, O'Donnell JB, Thrall JH, Keyes JWJ. Gallium-67 scintigraphy in untreated and treated non-Hodgkin lymphomas. *J Nucl Med* 1978;19:875–879.
22. Osman S, Danpure HJ. The use of 2-[18F]fluoro-2-deoxy-D-glucose as a potential in vitro agent for labeling human granulocytes for clinical studies by positron emission tomography. *Int J Rad Appl Instrum* 1992;19:183–190.
23. Kubota R, Yamada S, Kubota K, Ishiwata K, Tamahashi N, Ido T. Intratumoral distribution of fluorine-18-fluorodeoxyglucose in vivo: high accumulation in macrophages and granulocytes studied by microautoradiography. *J Nucl Med* 1992;33:1972–1980.
24. Kubota R, Yamada S, Kubota K, Ishiwata K, Tamahashi N, Ido T. Autoradiographic demonstration of 18F-FDG distribution within mouse FM3A tumour tissue in vivo. *Kaku Igaku* 1992;29:1215–1221.
25. Tahara T, Ichiya Y, Kuwabara Y, et al. High [18F]-fluorodeoxyglucose uptake in abdominal abscesses: a PET study. *J Comput Assist Tomogr* 1989;13:829–831.
26. Sulavik SB, Spencer RP, Castriotta RJ. Panda sign—avid and symmetrical radiogallium accumulation in the lacrimal and parotid glands. *Semin Nucl Med* 1991;21:339–340.
27. Kissane JM, ed. *Anderson's Pathology*. St. Louis, Baltimore, Philadelphia, Toronto: C.V. Mosby; 1990:978–981.
28. Caroit M. Bone and muscular lesions in sarcoidosis. *Ann Med Interne* 1984;135:102–104.
29. Wolfe SM, Pinais RS, Aelion JA, Goodman RE. Myopathy in sarcoidosis: clinical and pathologic study of four cases and review of the literature. *Semin Arth Rheum* 1987;16:300–306.
30. Patel N, Krasnow A, Sebastian JL, Collier BD, Hellman RS, Isitman AT. Isolated muscular sarcoidosis causing fever of unknown origin: the value of gallium-67 imaging. *J Nucl Med* 1991;32:319–321.